DOI: 10.1002/ejic.200800022

Formation of Micro/Macroporous Hierarchical Spheres of Titanosilicate Umbite

Víctor Sebastián,[a] Carlos Téllez,[a,b] Joaquín Coronas,*[a,b] and Jesús Santamaría[a,b]

Keywords: Zeolite analogues / Titanates / Umbites / Crystal growth / Microporous structures

Polycrystalline spheres of up to 2 mm diameter of microporous titanosilicate $K_2TiSi_3O_9{\cdot}H_2O$ with umbite structure (Ti-umbite) were prepared without the use of organic structuring agents. The spheres, while preserving the inherent microporosity of the umbite type-material, are organized as hierarchical materials with macropores in the 0.1–1.4-μm size range. Ti-umbite spheres were only produced by hydrothermal synthesis under rotation conditions, at 230 °C by using a solution with the following molar composition: $0.284\,K_2O/0.287\,Na_2O/SiO_2/0.095\,TiO_2$(anatase)$/30.8\,H_2O$, and it was observed that the synthesis time and the rotation speed of the autoclave influenced the particle size distribution. When the procedure was carried out at 30 rpm and for 48 h, the size of the Ti-umbite spheres adjusted well to a normal distribution, with a statistical mode of 492 ± 13 μm. Also, under these conditions the amount of unreacted TiO_2 anatase, which has a key role in the formation of the Ti-umbite spheres, was only 14.4 wt.-%.

Introduction

The performance of zeolitic materials is often limited by intracrystalline diffusion processes that result in a slow transport in the zeolite micropores. This is especially critical in the case of large zeolitic particles[1] and also when zeolites are used as catalytic materials in fast reactions. One way around this problem is to prepare zeolite crystals with a large aspect ratio, so that the length of the diffusion path is limited.[2] In a different approach, zeolites with hierarchical pore architectures containing micro and mesopores (or micro and macropores)[3] have been advocated as a solution to these problems, and hierarchical materials with micro/mesopores, meso/macropores, and micro/macropores have been successfully prepared. Generally, the control of the bimodal porosity is achieved by combining suitable organic templates for the required scale organization.[4] This combination usually requires two organic compounds: one for structuring the intrinsic microporosity of the material and another to create either the meso or macroporosity. This is the so-called dual templating method.[5,6] Other widely applied strategies for generating mesopores could involve steaming, acid-leaching, or alkaline desilication of previously prepared zeolite crystals.[7,8] Finally, hierarchical zeolites have also been produced by growing zeolite crystals around carbon particles[3] or by using mesoporous carbon prepared from carbohydrates as hard template[9] or natural materials, such as diatomite frustules[10] or columnar and discoid diatom,[11] as templates.

In a previous work, micrometric spheres of microporous titanosilicate umbite (Ti-umbite) having hierarchical pore systems were prepared by direct liquid-phase hydrothermal synthesis under a range of synthesis conditions in which a successful synthesis always required agitation by rotation and the use of TiO_2 anatase as a Ti source.[12] The micro/macroporous hierarchical architecture of these spheres was effective in reducing intraparticular transport resistances, as demonstrated for water and Sr^{2+} cations. Umbite is a microporous silicate mineral with the stoichiometry $K_2(Zr_{0.8}Ti_{0.2})Si_3O_9{\cdot}H_2O$.[13] Although its applications have not yet been widely studied, umbite, like the titanosilicates ETS-10 and ETS-4, possess framework structures built of MO_6 (M = Zr, Sn, Ti) octahedra and TO_4 (T = Si, Ge) tetrahedra.[14–17] These materials are good cation exchangers, and the ion-exchanged forms of Na^+ and Cs^+-Zr-umbite,[18] NH_4^+, Li^+, Na^+, K^+, Rb^+ and Cs^+-Ti-umbite,[19] and Cs^+ and Sr^{2+}-Sn-umbite[20] have been studied. Because of the one-dimensional eight-membered ring channel (ca. 5.5×2.7 Å), umbite-type materials do not adsorb N_2, although they are suitable for adsorbing small molecules, such as water (a slow reversible rehydration of the material has been reported[15]) and NH_3,[21] and to retain by ion exchange mono and divalent cations.[18–20] Recently, stannosilicate and titanosilicate umbite tubular membranes have shown good performance in the separation of H_2/N_2 mixtures achieving H_2/N_2 separation factors higher than 40.[22] Note as well that Ti-umbite silicates have in the past been called STS[19] and AM-2[15] materials.

[a] Department of Chemical and Environmental Engineering, University of Zaragoza,
50018 Zaragoza, Spain
Fax: +34-976-761879
E-mail: coronas@unizar.es
[b] Nanoscience Institute of Aragon, University of Zaragoza,
50009 Zaragoza, Spain

In spite of the interesting results obtained in our previous work,[12] the mechanism of formation of the hierarchically structured spheres remains unclear, and the key role of the operating conditions (presence of rotation, type of Ti precursor) needs to be clarified for this methodology to be extended to the preparation of other micro/macroporous systems. The present work explores these aspects by studying a wider range of conditions (regarding synthesis time and rotation speed) and by using a battery of characterization techniques to understand how the Ti-umbite crystals are assembled to produce solid spheres in which micropores and macropores are combined.

Results and Discussion

Hierarchical Pore System Spheres

As already mentioned, Ti-umbite spheres were only produced under rotation conditions.[12] In all the experiments carried out here, XRD analysis indicated that Ti-umbite was the only crystalline phase produced, together with some unreacted TiO_2 anatase. A second critical factor for the production of the spheres was the chemical composition of the starting synthesis solution: in particular the TiO_2/SiO_2 ratio has an important effect, so that below 0.021 (other parameters being constant) the composition gave rise only to crystals and not to spheres. A TiO_2/SiO_2 ratio of 0.095 was selected for this work, which produced good results as established in our precedent report.[12]

TiO_2 anatase was used before to synthesize titanosilicate ETS-10,[23,24] and depending on the conditions it was frequently detected by XRD in the final product as an unreacted material. Figure 1 compares the XRD pattern of pure Ti-umbite prepared by using $TiCl_3$ instead of TiO_2 and without any Na source[25] with those corresponding to spheres produced in 3–96 h, where a strong intensity corresponding to TiO_2 anatase appears. That is, XRD analysis reveals the presence of unreacted TiO_2 anatase, for which the intensity continuously decreases as a function of synthesis time, as depicted in Figure 2. XRD analysis was employed on the mixtures of TiO_2 anatase and pure Ti-umbite obtained with different synthesis times to obtain the relative amount of TiO_2 anatase remaining after synthesis. As can be inferred from Figure 2, the amount of remaining anatase initially decreases strongly with increasing synthesis time, but after 24–48 h of synthesis the proportion of unreacted TiO_2 anatase stayed at a constant level of around 14–15 wt.-%, and only after 96 h of hydrothermal synthesis was the amount of TiO_2 anatase lowered to 8.2 wt.-%. In contrast, it was already known that crystals collected together with the spheres exhibit a smaller amount of unreacted anatase than those within TiO_2 spheres.[12]

Figure 3 shows the particle size distributions of the Ti-umbite spheres as a function of synthesis time. To produce these representations, the dimensions of at least 120 particles of each experiment were measured by optical microscopy. The particles produced in 3 and 6 h experiments could not be analyzed because of the high amount of unreacted TiO_2 anatase. The mechanical stability of these samples was low, which resulted in a high proportion of fines. The distribution obtained was clearly unimodal (with a 492 ± 13 μm statistical mode, considering a Gaussian or normal distribution) only for spheres prepared at the optimum synthesis time of 48 h. Below this synthesis time, Figure 3 shows large spheres being formed after 12 h with Ti-umbite crystals probably nucleating around undissolved particles of TiO_2 anatase. These particles evolved to smaller spheres, probably through break-up during rotation, aided by the conversion of the TiO_2 trapped in the own spheres. Simultaneously, the formation of new spheres seems to be taking place, as indicated by the first peak of the histogram at 24 h, which later gives rise to the outlier observation at 36 h (at about 400 μm), and then the maximum of the histogram at 48 h. Note that the percentages of the unreacted TiO_2 anatase were 31.8, 14.8, and 14.4 wt.-% after 12, 24, and 48 h, respectively (see Figure 2). Of these data sets, only those corresponding to 36 and 48 h exhibit high enough normality test significance levels (0.08 and 0.15, respectively) to be considered following normal distributions, after performing the Shapiro–Wilk normality test (based on

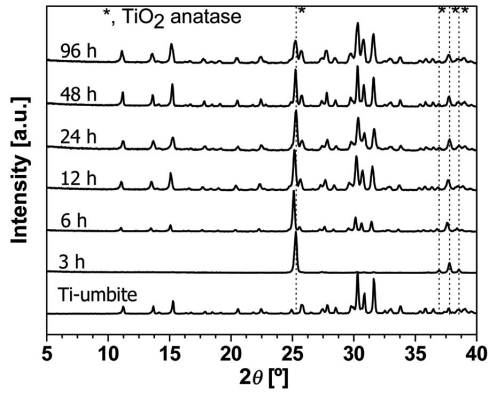

Figure 1. XRD patterns, from bottom to top, of pure Ti-umbite (prepared by using $TiCl_3$) and of crushed spheres prepared at a rotation speed of 30 rpm and different synthesis times.

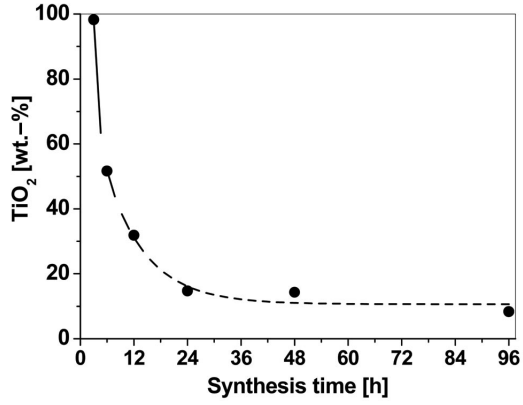

Figure 2. Unreacted TiO_2 anatase as detected (see Figure 1) and quantified by XRD in Ti-umbite spheres prepared at a rotation speed of 30 rpm as a function of synthesis time. A second-order exponential decay function was used as a guide for the eye.

a default significance level of 0.05). The others can be considered as random distributions. In contrast, the distribution at 48 h seems skewed toward larger particle sizes, so that a log-normal particle size distribution allows a better fitting to be obtained with a coefficient of determination ($R^2 = 0.93$) larger than that calculated for the normal distribution ($R^2 = 0.88$). Duplicating the synthesis time from 48 to 96 h yields a random distribution of sphere diameters where almost all sizes are represented, probably as a result of multiple growth, dissolution, and break-up processes. The differences in the distribution of particle sizes between the populations of spheres resulting from 48 and 96 h syntheses can readily be appreciated by direct visual observation, as shown by Figure 4, where a good correspondence between the appearance of the spheres and their diameter distributions is observed.

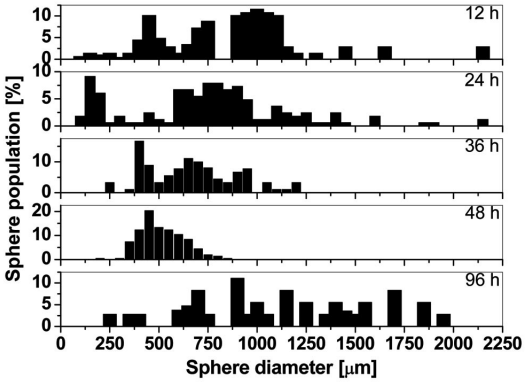

Figure 3. Size (diameter) distributions for Ti-umbite spheres prepared at a rotation speed of 30 rpm and different synthesis times.

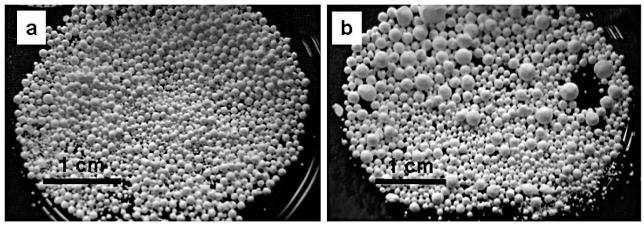

Figure 4. Digital camera images of Ti-umbite spheres prepared at a rotation speed of 30 rpm and synthesis times of 48 (a) and 96 h (b).

Together with the Ti-umbite spheres, Ti-umbite crystals were collected at the end of the synthesis. Figure 5 represents the weights of crystals, spheres, and crystals + spheres obtained as a function of synthesis time in an autoclave volume of 35 mL (see Experimental Section). The total amount of Ti-umbite material was kept approximately constant at 2200 mg for any synthesis time. However, Figure 5 clearly shows that the proportion of spheres continuously increased with synthesis time at the expense of crystals, which suggests a mechanism in which spheres grow by the incorporation of crystals and more likely of nutrients coming from the dissolution of crystals.

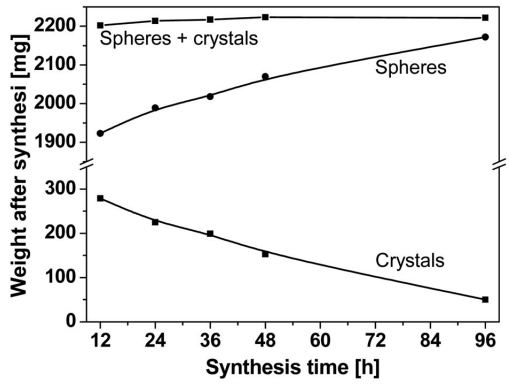

Figure 5. Weights of crystals, spheres, and crystals + spheres obtained at 30 rpm as a function of synthesis time achieved in an autoclave volume of 35 mL, as described in the Experimental Section.

Because rotation is critical (Ti-umbite spheres were only produced under agitation conditions), it could be expected that rotation speed modifies the particle size distribution. This is indeed the case, as shown in Figure 6 for spheres prepared with 96 h long hydrothermal syntheses. Although this synthesis time produces the random distribution already discussed at low rotation speeds, when the rotation speed increased from 15–30 to 60 rpm the resulting population of sphere diameters could be fit by a normal distribution, with a normality test significance level value of 0.04. Simultaneously, the sphere diameters diminished, which suggests acceleration in the above-mentioned growth and dissolution processes.

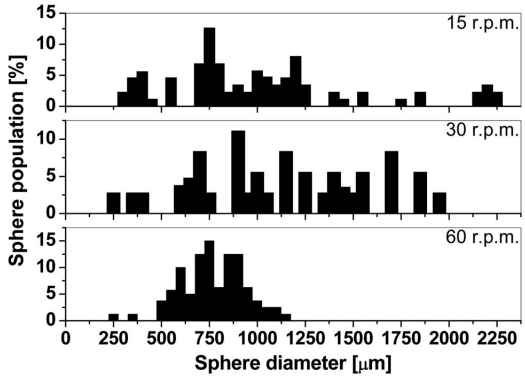

Figure 6. Particle size distributions for Ti-umbite spheres prepared at 96 h and different rotation speeds.

Micro/Macroporous Hierarchical Spheres

Figure 7 shows SEM images of cross sections of Ti-umbite spheres obtained at 30 rpm and 12–48 h that where embedded in resin and subsequently polished. These cross sections reveal intergrowths, both in the middle and in the periphery, which leaves behind visible macropores. Note that the appearance of the spheres in Figure 7 is partly modified by the resin itself. Thus, in Figure 7a, c, e, and g prepared at 12, 24, 48, and 96 h the spheres have diameters

of 1390, 790, 600, and 1840 μm, respectively. In small spheres the resin penetrates easily and is present throughout the particle, whereas for the larger diameters there is a lower penetration of the resin into the macroporosity. This can be clearly appreciated in Figure 7a and g, where the larger spheres present a clear resin–crystals annulus; the crystals in the middle are grazed by the polishing operation. The resin reinforces the sphere for the polishing, and this is the reason why the smaller spheres of 600 μm, in which the resin was embedded in the whole particle, seem to have flatter surfaces. In any case, crystal intergrowths are appreciable for all four sphere sizes, and they can be considered as polycrystalline spheres, although intergrowth becomes more extended at high synthesis times: compare Figure 7f and h at 48 and 96 h, respectively, with Figure 7b and d at 12 and 24 h, respectively.

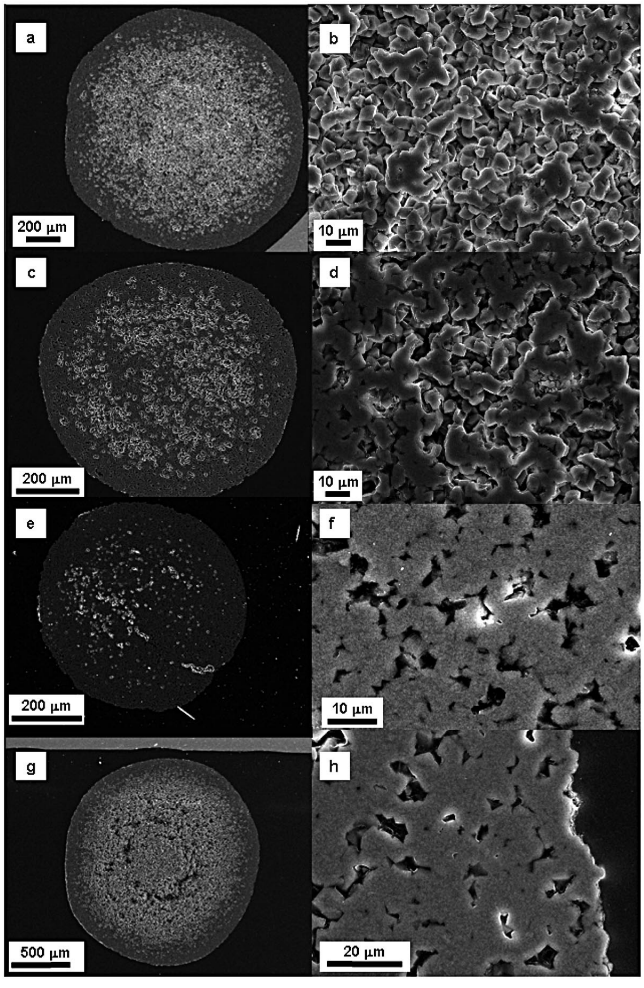

Figure 7. SEM images of cross sections (after embedding in resin and subsequent polishing) of Ti-umbite spheres as obtained at 30 rpm after: (a, b) 12 h; (c, d) 24 h; (e, f) 48 h; (g, h) 96 h.

Together with the Ti-umbite spheres, Ti-umbite crystals were collected at the end of the synthesis (Figure 8). In general, these crystals are considerably larger than those constituting the polycrystalline spheres quoted in Table 1, although this difference in size is more noticeable at the highest synthesis time of 48 h when single crystals reach almost 20 μm in length (Figure 8d), whereas crystals in the spheres are around 5.5–6.5 μm in length. Figure 8e corresponds to crystals recovered after 96 h (in a smaller amount, see Figure 5), whose sizes are clearly smaller, in good accordance with the dissolution process before envisaged at longer synthesis times. Table 1 also shows that crystals from the periphery of the spheres may be larger than those in their middles, which indicates that in the growing surface of the spheres the availability of nutrients would be higher. Anyway, this statement should be taken with caution, as the confidence intervals often overlap. To calculate these average values, at each synthesis time, more than 30 crystals were considered in spheres of different diameter, and no significant variations where found from one sphere to the other.

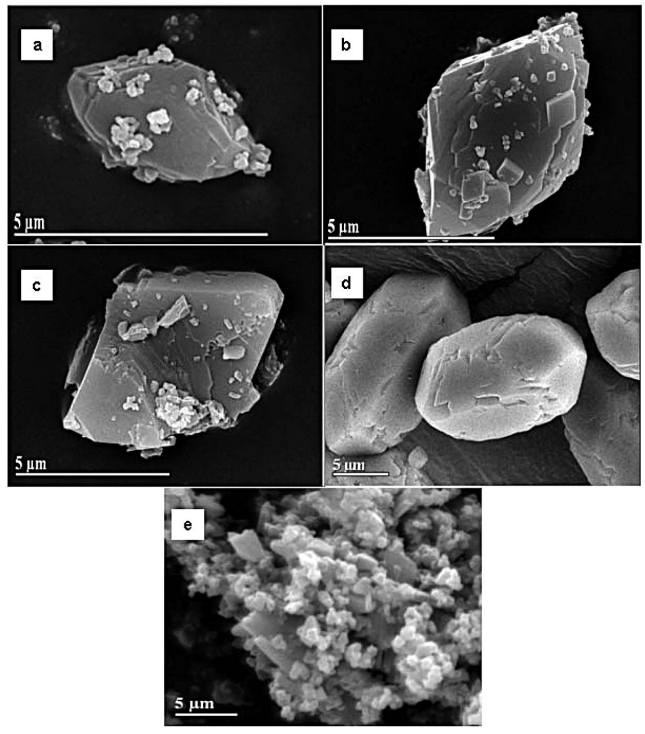

Figure 8. SEM images of single Ti-umbite crystals collected together with the spheres in 30 rpm syntheses at: (a) 6 h, (b) 12 h, (c) 24 h, (d) 48 h, and (e) 96 h.

Table 1. Average sizes of crystals constituting the polycrystalline spheres as a function of synthesis time at 30 rpm.

Synthesis time [h]	Length [μm]		Width [μm]	
	Middle	Periphery	Middle	Periphery
6	3.4 ± 0.0	3.4 ± 0.0	2.1 ± 0.1	2.2 ± 0.1
12	6.0 ± 0.8	6.7 ± 0.2	4.0 ± 0.5	4.4 ± 0.7
24	6.2 ± 0.3	6.6 ± 0.2	3.9 ± 0.3	4.2 ± 0.5
48	5.5 ± 0.2	6.5 ± 0.5	3.8 ± 0.1	4.2 ± 0.3
96	6.5 ± 0.5	6.4 ± 0.6	5.0 ± 0.4	4.6 ± 0.7

The Hg intrusion microporosimetry confirms (Figure 9) the presence in the spheres of macropores of two different sizes: 0.1–0.4 and 1.3–1.4 μm. These macropores give rise to the hierarchical micro/macroporous structures of the Ti-umbite spheres prepared with the micropores belonging in-

trinsically to the umbite material. The cumulative Hg intrusion also shows a small amount of larger macropores (around 10–25 μm) and the total absence of mesopores. From Hg intrusion porosities of 40 and 23% were obtained for the spheres obtained at 12 and 48 h of hydrothermal synthesis, respectively. The reduction of the porosity as a function of synthesis time would be associated to the aforementioned TiO_2 anatase conversion and the reorganization of the material in the sphere. This reduction in porosity would give rise to the filling of 1.3 μm pores in the 12 h spheres to produce 0.2–0.4 μm pores in the 48 h spheres. Finally, in these intrusion experiments, the Hg pressure reached values of up to 4000 bar without breaking the spheres, which shows their mechanical strength.

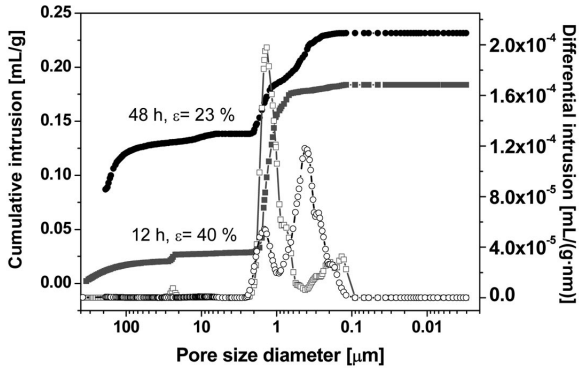

Figure 9. Hg cumulative intrusion and pore size distribution of Ti-umbite spheres prepared at 30 rpm and 12 (grey) and 48 (black) h of hydrothermal synthesis.

Finally, we hypothesize that the rotation conditions allows the aggregation/ensemble of the species in the precursor gel into, first, spheres of low crystallinity (in terms of the product umbite), perhaps through a centrifugal effect that would join together particles on the internal surface of the autoclave. As it is shown in Figure 5, the total amount of solid material (spheres and crystals) collected kept approximately constant for synthesis times ranging from 12 to 96 h. This observation indicates that, because of lack of reactants, the gel became unable to produce more solids after 12 h, and in consequence, all the aforementioned changes in TiO_2 anatase conversion (Figure 2) and diameter distributions (Figure 3) are caused by the reorganization of these solids. This reorganization would involve the incorporation of crystals into spheres (directly or through dissolution) and the production of more compact spheres (Figure 9). Both situations would reduce the exposed area (and the rate of dissolution, which, for a given supersaturation, increases with the crystal area) of any solid in the synthesis medium. As a result, a pseudoequilibrium is established that translates into the observation of a normal distribution (Figure 3, 48 h; Figure 6, 60 rpm). Any of these processes would be accelerated by the increasing rotation speed, which would reduce concentration gradients through the autoclave.

Conclusions

Polycrystalline spheres of up to 2 mm diameter of microporous titanosilicate $K_2TiSi_3O_9{\cdot}H_2O$ with umbite structure can be prepared by liquid-phase hydrothermal synthesis without resorting to the use of organic structuring agents. The synthesis of these spheres always requires agitation by rotation and the use of TiO_2 anatase as a Ti source. This Ti precursor seems to have a key role in the formation of the spheres, favoring the nucleation of the titanosilicate and perhaps the subsequent intergrowth and aggregation into spheres. Unreacted TiO_2 anatase is detected by X-ray diffraction in the products recovered at the end of the hydrothermal synthesis. The lowest amount of unreacted TiO_2 anatase detected in the Ti-umbite spheres was 8.2 wt.-% after 96 h of synthesis. The rotation speed and the synthesis time influence the sphere diameter distribution, which under certain conditions (30 rpm and 36–48 h) is in practice normal. From the point of view of the diameter distribution and of the amount of unreacted TiO_2 anatase, 48 h and 30 rpm could be considered as an optimum synthesis time.

Hg porosimetry allows us to establish a sphere macroporosity in the 0.1–1.4 μm range, and the macropores are also evidenced by scanning electron microscopy. Finally, by working under rotation conditions and by using low-solubility nanometric-size precursors as the key components of the synthesis solution, this strategy could perhaps be extended to the preparation of other hierarchically structured nanoporous systems.

Experimental Section

General: Ti-umbite macroporous spheres were prepared by using the following molar composition: $0.284K_2O/0.287Na_2O/SiO_2/0.095TiO_2/30.8H_2O$. The precursor reactants were TiO_2 anatase (99.9 wt.-%, Aldrich), KOH (85 wt.-%, Merck), KCl (99 wt.-%, Panreac), and sodium silicate solution (25.5–28.5 wt.-% SiO_2, 7.5–8.5 wt.-% Na_2O, Merck). To prepare the precursor gel (37.54 g), KCl (0.990 g) and KOH (1.010 g) were dissolved in deionized water (22.78 g). Then, TiO_2 anatase (0.424 g) was added whilst stirring the above solution. After approximately 30 min of stirring, a homogeneous dispersion was produced. This stage is critical to avoid precipitation after the next step in which the sodium silicate solution (12.34 g) was mixed with the precedent solution. Then, after 60 min more of stirring, a white, nonviscous solution was obtained. This was poured into a Teflon-lined autoclave, which filled approximately 90% of its volume (35 mL), and hydrothermal synthesis was then carried out at 230 °C for 3–96 h. The autoclave was horizontally rotated (15, 30, or 60 rpm) during synthesis. When the synthesis was finished by quenching the autoclave in water, a mixture of polycrystalline spheres and single crystals was obtained. The spheres remained at the bottom of the autoclave, while crystals were separated from the dispersion by filtration, by washing with deionized water at room temperature, and by drying overnight at 100 °C. Also, for comparison, Ti-umbite powder was prepared by using fumed silica as SiO_2 source, that is, without Na in the gel composition, and $TiCl_3$ instead of TiO_2 with a molar composition of $5.3\ K_2O/3.6\ SiO_2/TiO_2/120\ H_2O$.[25] Note that that all the materials in this work were prepared without the use of organic structuring agents.

The Ti-umbite products were characterized by scanning electron microscopy (SEM, JEOL JSM-6400) and X-ray diffraction (XRD, Philips X'pert MPD diffractometer by using Cu-K_α radiation). Hg intrusion porosimetry was performed with a Micromeritics Auto-Pore IV.

Acknowledgments

Financing from the Spanish Ministry of Education and Science (MAT2004-02184) is gratefully acknowledged.

[1] C. C. Pavel, W. Schmidt, *Chem. Commun.* **2006**, 882–884.
[2] M. A. Ulla, E. Miro, R. Mallada, J. Coronas, J. Santamaria, *Chem. Commun.* **2004**, 528–529.
[3] M. Hartmann, *Angew. Chem. Int. Ed.* **2004**, *43*, 5880–5882.
[4] B. Zhang, S. A. Davis, S. Mann, *Chem. Mater.* **2002**, *14*, 1369–1375.
[5] B. T. Holland, L. Abrams, A. Stein, *J. Am. Chem. Soc.* **1999**, *121*, 4308–4309.
[6] S. A. Davis, S. L. Burkett, N. H. Mendelson, S. Mann, *Nature* **1997**, *385*, 420–423.
[7] S. van Donk, A. H. Janssen, J. H. Bitter, K. P. de Jong, *Catal. Rev.* **2003**, *45*, 297–319.
[8] J. C. Groen, J. A. Moulijn, J. Perez-Ramirez, *J. Mater. Chem.* **2006**, *16*, 2121–2131.
[9] K. Zhu, K. Egeblad, C. H. Christensen, *Eur. J. Inorg. Chem.* **2007**, 3955–3960.
[10] O. Hernandez-Ramirez, P. I. Hill, D. J. Doocey, S. M. Holmes, *J. Mater. Chem.* **2007**, *17*, 1804–1808.
[11] X. Cai, G. S. Zhu, W. W. Zhang, H. Y. Zhao, C. Wang, S. L. Qiu, Y. Wei, *Eur. J. Inorg. Chem.* **2006**, 3641–3645.
[12] V. Sebastian, I. Diaz, C. Tellez, J. Coronas, J. Santamaria, *Adv. Funct. Mater.*, DOI: 10.1002/adfm.200701067.
[13] G. D. Ilyushin, *Inorg. Mater.* **1993**, *29*, 1128–1133.
[14] D. M. Poojary, A. I. Bortun, L. N. Bortun, A. Clearfield, *Inorg. Chem.* **1997**, *36*, 3072–3079.
[15] Z. Lin, J. Rocha, P. Brandao, A. Ferreira, A. P. Esculcas, J. D. Pedrosa de Jesus, *J. Phys. Chem. B* **1997**, *101*, 7114–7120.
[16] Z. Lin, J. Rocha, A. Valente, *Chem. Commun.* **1999**, 2489–2490.
[17] J. Plevert, R. Sanchez-Smith, T. M. Gentz, H. Li, T. L. Groy, O. M. Yaghi, M. O'Keeffe, *Inorg. Chem.* **2003**, *42*, 5954–5959.
[18] S. R. Jale, A. Ojo, F. R. Fitch, *Chem. Commun.* **1999**, 411–412.
[19] B. Mihailova, V. Valtchev, S. Mintova, L. Konstatinov, *J. Mater. Sci. Lett.* **1997**, *16*, 1303–1304.
[20] P. Pertierra, M. A. Salvado, S. García-Granda, S. A. Khainakov, J. R. García, *Thermochim. Acta* **2004**, *423*, 113–119.
[21] N. Navascues, E. D. Skouras, V. Nikolakis, V. N. Burganos, C. Tellez, J. Coronas, *Chem. Eng. Process.*, DOI: 10.1016/j.cep.2007.05.025.
[22] V. Sebastián, Z. Lin, J. Rocha, C. Téllez, J. Santamaría, J. Coronas, *Chem. Commun.* **2005**, 3036–3037.
[23] J. Rocha, A. Ferreira, Z. Lin, M. W. Anderson, *Microporous Mesoporous Mater.* **1998**, *23*, 253–263.
[24] X. Yang, J. L. Paillaud, H. F. W. J. van Breukelen, H. Kessler, E. Duprey, *Microporous Mesoporous Mater.* **2001**, *46*, 1–11.
[25] V. Sebastian, Z. Lin, J. Rocha, C. Tellez, J. Santamaria, J. Coronas, *Chem. Mater.* **2006**, *18*, 2472–2479.

Received: January 8, 2008
Published Online: April 11, 2008

